



**CHALMERS**  
UNIVERSITY OF TECHNOLOGY

## Spontaneous Charge Separation at the Metal-Water Interface

Downloaded from: <https://research.chalmers.se>, 2026-04-04 14:54 UTC

Citation for the original published paper (version of record):

Svensson, R., Grönbeck, H. (2024). Spontaneous Charge Separation at the Metal-Water Interface. *ChemPhysChem*, 25(8). <http://dx.doi.org/10.1002/cphc.202400099>

N.B. When citing this work, cite the original published paper.

# Spontaneous Charge Separation at the Metal-Water Interface

Rasmus Svensson\*<sup>[a]</sup> and Henrik Grönbeck\*<sup>[a]</sup>

Reactions at the metal-water interface are essential in a range of fundamental and technological processes. Using Density Functional Theory calculations, we demonstrate that water substantially affects the adsorption of H and O<sub>2</sub> on Cu(111), Ag(111), Au(111), Pd(111) and Pt(111). In water, H is found to undergo a spontaneous charge separation, where a proton desorbs to the water solution while an electron is donated to the surface. The reaction is exothermic over Au and Pt and associated with low barriers. The process is facile also over Pd, albeit slightly endothermic. For O<sub>2</sub>, water is found to increase

the metal-to-adsorbate charge transfer, enhancing the adsorption energy and O–O bond length as compared to the adsorption in the absence of water. The magnitudes of the effects are system dependent, which implies that calculations should treat water explicitly. The results elucidate previous experimental results and highlights the importance of charge-transfer effects at the metal-water interface; both to describe the potential energy landscape, and to account for alternative reaction routes in the presence of water.

## Introduction

Many heterogeneous catalytic reactions are performed over transition metal particles, with reaction conditions varying from high temperatures and pressures with the reactants and products in the gas-phase, to low temperatures with solvated reactants and products.<sup>[1]</sup> The detailed understanding of metal-gas processes has developed rapidly over the past decades thanks to experimental techniques with in situ capabilities<sup>[2]</sup> combined with the possibility to do electronic structure calculations with sufficient accuracy.<sup>[3–8]</sup> The understanding of reactions at the metal-liquid interface is not as developed as reactions at the metal-gas interface.<sup>[9]</sup> This is unfortunate given the many sustainable energy applications occurring at this interface, such as electrolysis of water for H<sub>2</sub> production,<sup>[10]</sup> proton-exchange membrane fuel cells,<sup>[11]</sup> and synthesis of fuels and chemicals.<sup>[12]</sup>

The presence of a liquid solution can affect heterogeneous catalytic reactions in different ways, resulting in modified potential energy landscapes and, consequently, altered turnover frequencies and selectivities.<sup>[13–17]</sup> The solvent may influence the reaction kinetics in a direct way by competitive adsorption<sup>[18]</sup> and modification of reaction rates due to the

solvent reorganization close to the metal surface during elementary reactions.<sup>[19]</sup> A liquid solvent may also, via e.g. hydrogen bonds, influence the stability of certain intermediates<sup>[20]</sup> and elementary reaction rates.<sup>[21]</sup> The stabilization of certain intermediates could, for example, influence the selectivity of reactions, such as direct hydrogen peroxide formation, where the desorption of the partially reduced species (H<sub>2</sub>O<sub>2</sub>) should be favored over further reduction to H<sub>2</sub>O.<sup>[22,23]</sup> Furthermore, the solvent may take part in the reaction by enabling new reaction pathways. Adsorbed solvent species could act as a hydrogen donor in hydrogenation reactions.<sup>[17]</sup> The solvent could also mediate the transfer of hydrogen to various reaction intermediates.<sup>[17,23]</sup> Similar to a direct transfer mechanism is the desorption of hydrogen to the solution forming solvated protons.<sup>[24–28]</sup>

Electronic structure calculations targeting reactions at the metal-liquid interface have in the past sometimes been performed omitting the effect of the solution. Implicit solvation models is a first step to account for the influence of the liquid on adsorption energies, although such models do not accurately describe effects of charge-transfer and hydrogen bonds.<sup>[29]</sup> In the case of water, computational studies have recently shown that explicit treatment of water molecules require the inclusion of more than a few water molecules to converge adsorption energies.<sup>[29,30]</sup> Explicit treatment of water is computationally demanding due to the flexibility of liquid water with many close-lying minima on the potential energy surface.

Here, we explore the effects of the metal-water interface for H and O<sub>2</sub> adsorption on the (111) surfaces of Cu, Ag, Au, Pd and Pt. The systems are prototypical and relevant within, for example, the production of fuels, and fuel-cell technology. The potential energy surfaces are mapped using density functional theory (DFT) calculations in the presence and absence of water. *Ab initio* molecular dynamics (AIMD) simulations are performed to find the global minima of the water structures. We find that adsorption at the metal-water interface gives rise to significant

[a] R. Svensson, H. Grönbeck  
Department of Physics and Competence Centre for Catalysis,  
Chalmers University of Technology,  
SE-412 96 Göteborg, Sweden  
E-mail: rassve@chalmers.se  
ghj@chalmers.se

Supporting information for this article is available on the WWW under <https://doi.org/10.1002/cphc.202400099>

© 2024 The Authors. ChemPhysChem published by Wiley-VCH GmbH. This is an open access article under the terms of the Creative Commons Attribution Non-Commercial License, which permits use, distribution and reproduction in any medium, provided the original work is properly cited and is not used for commercial purposes.

charge separation effects. Adsorbed H undergoes a redox reaction in the presence of water, where a proton desorbs into the solution, whereas an electron is left in the surface. The process is exothermic over Ag, Au and Pt, whereas it is close to thermo-neutral over Pd and endothermic over Cu. The barrier for proton desorption is low over Au and Pt, whereas it is about 0.6 eV over Pd and 0.7 eV over Ag. Water is found to significantly affect also O<sub>2</sub> adsorption via hydrogen bonds, promoting a metal-to-O<sub>2</sub> charge transfer, which increases the adsorption strength and O–O bond length. The charge separation at the metal-water interface is different in character for H compared to O<sub>2</sub>. H<sup>+</sup> is solvated in water, whereas charged O<sub>2</sub> is adsorbed on the surface. The results explain and rationalize the experimentally observed<sup>[31]</sup> charge separation effects at the metal-water interface. The spontaneous solvation of H<sup>+</sup> and metal-to-O<sub>2</sub> charge transfer have important consequences for the understanding of catalytic reactions, as it modifies the potential energy landscapes and enables alternative reaction pathways.

## Results

The effect of water on the adsorption properties of H and O<sub>2</sub> on the (111) surfaces of Cu, Ag, Au, Pd and Pt is investigated by comparing adsorption properties with and without water. H may in the presence of water be adsorbed on the surface or solvated in the water as a hydronium ion. The many hydrogen bonds in the presence of water makes the potential energy landscape complex with several minima, which are sampled by *ab initio* MD simulations. Atomic models of the different systems with Pt(111) are shown in Figure 1.

### Comparison between adsorbed H and water solvated H<sup>+</sup>

To compare the situations with H either being adsorbed on the surface or solvated in the water solution, H is initially placed on the metal (111) surface below the water solution or in the water solution. We do not observe any interchange between the two states during the 10 ps simulations. The charge states of H are clearly different depending on the mode of adsorption. A significant charge separation occurs when H is placed in the water solution. H is in this case in the form of a positively charged proton (H<sup>+</sup>) and the metal surface is negatively charged by e<sup>-</sup>. The charge state is for H adsorbed on the surface close to neutral (Au, Pt) or slightly negatively charged (Cu, Ag, Pd).

The energy of two trajectories with H adsorbed on the metal (red) or in the water solution (blue), are shown in Figure 2. Over Cu, the energies of the two trajectories are similar during the AIMD simulations. The charge separated state with H<sup>+</sup> in the water solution is over Ag and Au significantly lower in energy than H adsorbed on the surface. For Pd, the energies for the two states are similar and for Pt, the MD simulations indicate that H is preferably located in the solution,

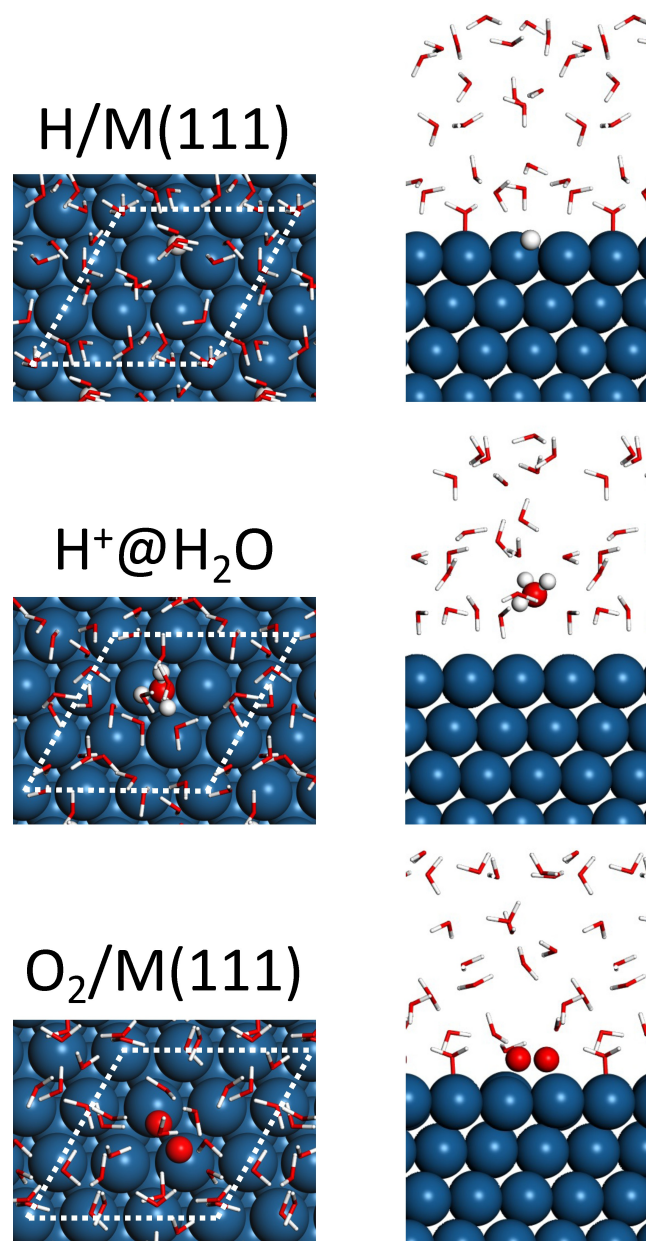


**Figure 1.** Atomic models with adsorption on Pt(111) in the presence of water. H adsorbed on the surface (top), H<sub>3</sub>O<sup>+</sup> and an electron in the surface (middle), and O<sub>2</sub> adsorbed on the surface. The systems are shown in top (left) and side (right) views. The surface cell is indicated by white dashed lines. Atomic color codes: Pt (blue), O (red) and H (white).

albeit, the energy preference over H adsorbed on the surface is not as pronounced as for Ag and Au.

The lowest energy configurations from the AIMD simulations are extracted and relaxed to obtain minimum energy configurations. The adsorption energies for H on the surface and H<sup>+</sup> solvated in the water are shown in Figure 3. As references, the adsorption energies of H over the bare (111) surfaces (no water solution) are presented. The tabulated values and additional information about the AIMD simulations are presented in the Supporting Information (SI).

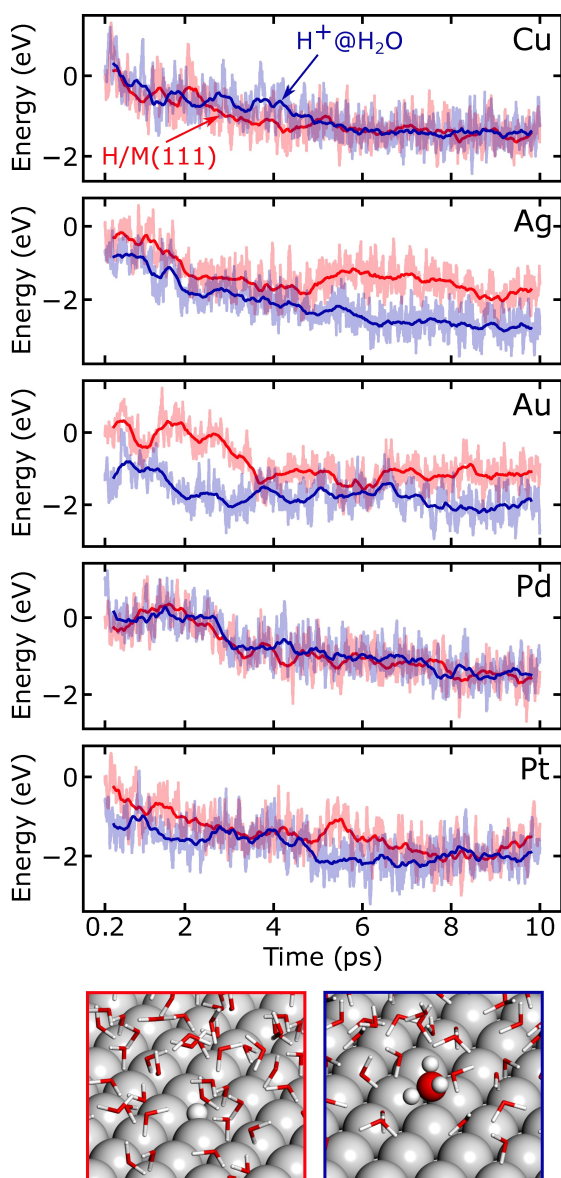


**Figure 2.** AIMD simulations for H adsorbed on the surface [red] and  $H^+$  residing in the water solution (with a negatively charged metal surface) [blue] over Cu(111), Ag(111), Au(111), Pd(111) and Pt(111). The AIMD simulations are performed over 10 ps. The bright trajectories show the energies obtained from the AIMD simulations, whereas the bold lines represent a 0.4 ps running average. The first 0.2 ps of the AIMD simulations are removed to avoid the high energies obtained from the starting configurations.

On a bare Cu(111) surface, H adsorption is exothermic. The presence of water makes the adsorption close to thermo-neutral. The charge separated state (water solvated  $H^+$  and a negatively charged metal surface) is endothermic, both with respect to gas phase  $H_2$  and H adsorbed on the surface. H adsorption is calculated to be endothermic on bare Ag(111) and Au(111). The effect of water on the adsorbed state is negligible for Ag, whereas the presence of water makes H adsorption slightly exothermic on Au. Solvation of H in the water forming  $H^+$  and a negatively charged metal surface is strongly exothermic on both Ag and Au. The increased

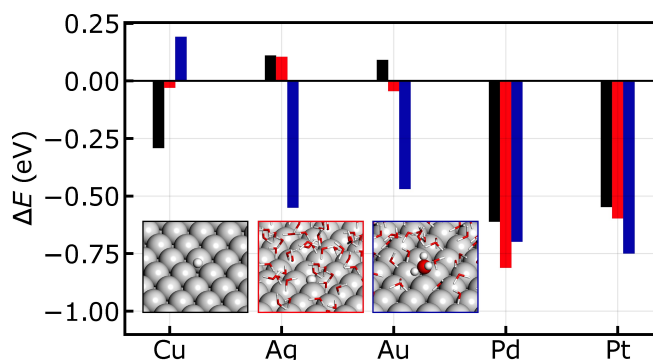


**Figure 3.** The adsorption energy of H on the bare surfaces (black), the adsorption energy of H on the surface in the presence of water (red) and the energy of  $H^+$  solvated in the water solution (blue). In the presence of water, the reference energy is an optimized water structure over the metal and  $1/2 H_2$ . The reference energy in the absence of water is the bare surface and  $1/2 H_2$ .

adsorption strength of H on Au in the presence of water is in agreement with previous TPD experiments over Au(111).<sup>[32]</sup> On Pd(111), the adsorption energy of H is strong, which is further increased in the presence of water. A separation of charge with solvated  $H^+$  is slightly unfavorable with respect to adsorbed H on Pd. However, the charge separated state is clearly exothermic with respect to gas phase  $H_2$ . On Pt(111), the adsorption energy of H is only slightly affected by the presence of water. However, in contrast to Pd, the water solvated  $H^+$  is exothermic with respect to H adsorbed on the surface.

The high stability of the charge separated state for Ag, Au, Pd and Pt is related to the high work functions of these metals<sup>[33]</sup> in combination with the high solvation energy of  $H^+$ .<sup>[34]</sup> It should be noticed that the stability of a water solvated  $H^+$  and an excess electron in the metal surfaces is not solely determined by the work function of the metal measured in vacuum. In vacuum, the trend of the work functions are  $\phi_{Pt} > \phi_{Pd} > \phi_{Au} > \phi_{Cu} > \phi_{Ag}$ ,<sup>[33]</sup> which is slightly different from the stability of the charge separated states. The discrepancy can be traced to the influence of water; the work-functions are reduced with different amounts in the presence of water<sup>[35]</sup> and the water structures for the two cases are different across the metals.

The *ab initio* molecular dynamics simulations together with the adsorption energies of the relaxed structures show that charge separation forming solvated  $H^+$  is energetically preferred (Ag, Au, Pt) or comparable (Pd) with the state of adsorbed H in the presence of water. To study possible kinetic limitations of the charge separation process ( $H_{ads} + H_2O_{solution} \rightarrow H_3O_{solution}^+ + e_{metal}^-$ ), we perform constrained AIMD simulations using the blue-moon ensemble method<sup>[36]</sup> to obtain free energy barriers. The constrain is the H-H<sub>2</sub>O bond distance (specifically, the bond length between the H that is transferred and the oxygen atom in the water molecule). The details of the procedure and an error analysis are described in the SI.

The free energy barrier for charge separation is 0.85 eV over Cu(111). The high barrier is consistent with the energies presented in Figure 3, where the charge separation is clearly

endothermic. The free energy barrier is 0.68 eV on Ag(111), although the process is clearly exothermic (see Figure 3). The barrier is in the case of Ag related to the large distortion of the water structure required for the  $H^+$  transfer.

The situation is different over Au(111), where the reaction has a free energy barrier of only 0.28 eV. H adsorbs strongly on the Pd(111) surface, and the  $H^+$  transfer is associated with a free energy barrier of 0.58 eV. The barrier over Pt(111) is similar to Au(111), being only 0.42 eV. The calculated free energy barriers are close to the estimated electronic energy barriers obtained from the constrained AIMD simulations, where the H–H<sub>2</sub>O bond length is linearly decreased during 5 ps (see SI). The similarity between the free and electronic energy barriers reflects the small difference in entropy between the initial and transition states.

The maximum energy along the transfer of  $H^+$  to the solution, is when the hydrogen atom on the surface has moved from the initial hollow site to an atop site below a water molecule. It should be noted that the free energy barriers are influenced by the initial orientation of the water molecule that accepts the  $H^+$  forming  $H_3O^+$ . Thus, the barriers could be lower with other transfer paths. The constrained AIMD simulations suggest that charge separation is facile, forming solvated  $H^+$  and a negatively charged metal surface.

The facile and exothermic charge separation at the metal-water interface rationalizes the experimental finding that Au, Pd and Pt-alloy nanoparticles are charged during direct hydrogen peroxide formation.<sup>[27]</sup> That the charge separation process is facile over Pt agrees with early single crystal experiments<sup>[31]</sup> where H and H<sub>2</sub>O were co-adsorbed on Pt(111). Upon heating the sample, an initial decrease in the metal work function was recorded prior to H<sub>2</sub>O desorption, associated with solvation of  $H^+$ . Moreover, the IR-experiments monitored the vibrational signatures of  $H_3O^+$ .<sup>[31]</sup> Importantly, the experiments in Ref. [31] did not observe  $H^+$  transfer over a Cu(110) surface, which agrees with the calculated endothermicity of this reaction (Figure 4).

The possibility of charge separation mechanisms and reaction paths involving  $H^+$  transfer via H<sub>2</sub>O has previously been discussed for different hydrogenation reactions.<sup>[17,23,26,37]</sup> Barriers have been reported for local shuttle mechanisms where a surface-bound H is transferred to a reaction intermediate over one water molecule acting as a bridge. Here we show that long-ranged H-transfer with complete charge separation is possible over a range of metal systems.

### Water-induced charge separation upon O<sub>2</sub> adsorption

The presence of water also influences the adsorption properties of O<sub>2</sub>, see Figure 5, where the results for the cases with and without water are presented. O<sub>2</sub> dissociates spontaneously when adsorbed on a water covered Cu(111), and the results for Cu are therefore only presented in the SI. The figure reports electronic energies, however, the trends are similar for free adsorption energies. The entropy contributions to the free energy are similar for the bare and water covered surfaces, as

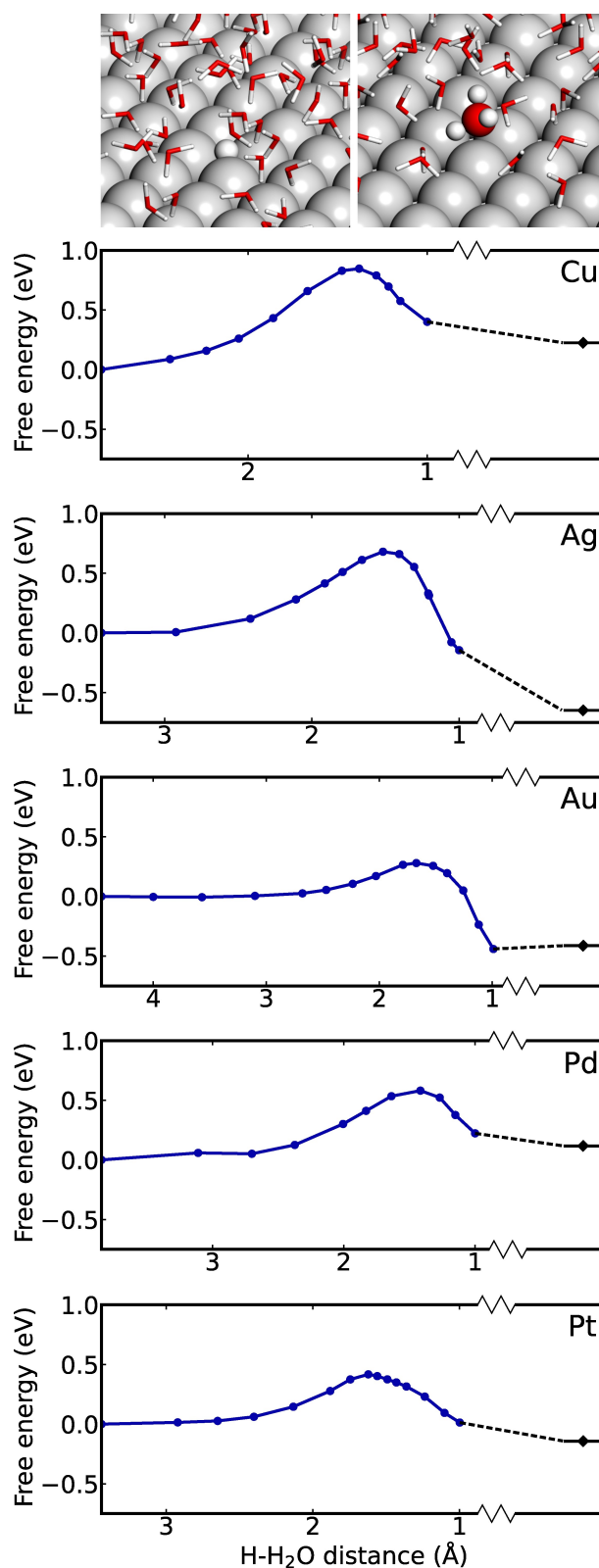


**Figure 4.** Free energy barriers for the charge separation process, where the adsorbed hydrogen leaves the surface to the water solution as a proton while the excess electron is donated to the surface, over Cu(111), Ag(111), Au(111), Pd(111) and Pt(111). The free energy gradients are obtained from blue-moon sampling for 11–15 different H–H<sub>2</sub>O bond lengths. The free energy landscape is obtained by integrating the gradients along the reaction coordinate (H–H<sub>2</sub>O bond length). The structure with H adsorbed on the surface is set as reference. The black lines indicate the free energies obtained from optimized structures and vibrational analyses (Figure 3).

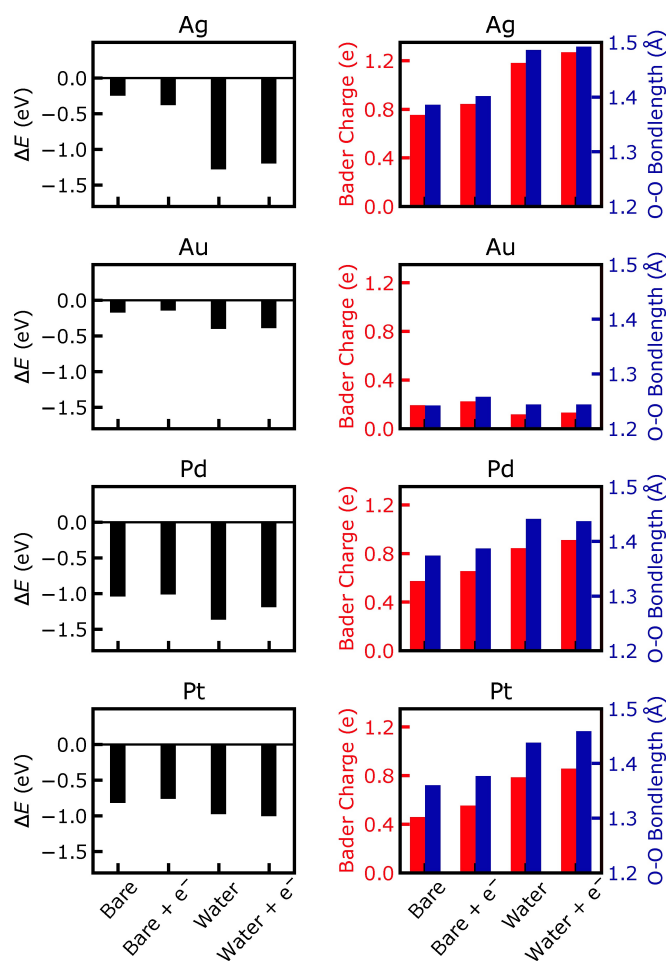


**Figure 5.** The adsorption properties of  $O_2$  over Ag(111), Au(111), Pd(111) and Pt(111) in the absence and presence of water. Results are also presented for  $O_2$  adsorption with an excess electron in the system. Left: The zero-point corrected adsorption energy and Right: The excess Bader charge of  $O_2$  and O–O bond length.

the vibrational modes of adsorbed H and  $O_2$  are only weakly affected by water.

The adsorption energy of  $O_2$  on Ag(111) is strongly enhanced ( $\sim 1$  eV) in the presence of water. The enhanced adsorption strength correlates with an increased metal-to- $O_2$  electron transfer. The excess Bader charge on  $O_2$  is 0.75 e in the absence of water and 1.18 e in the presence of water. The enhanced charge transfer results in a further elongation of the O–O bond length from 1.39 Å to 1.49 Å. (The gas-phase O–O bond length is calculated to be 1.23 Å.) The enhanced adsorption strength and charge transfer is a consequence of the hydrogen bonds between the adsorbed  $O_2$  and the water molecules. The hydrogen bonds elongate the O–O bond, which facilitates charge transfer, thus further increasing the strength of the hydrogen bonds.

$O_2$  is weakly adsorbed on Au(111), with only a small charge transfer between the surface and the molecule. The adsorption energy increases by  $\sim 0.2$  eV in the presence of water. The minor effect of water for the  $O_2$  adsorption energy on Au(111) is

consistent with small changes in the Bader charge and O–O bond length, respectively.

$O_2$  adsorbs strongly on bare Pd(111), with an adsorption energy of about 1 eV. The excess Bader charge and O–O bond length are 0.6 e and 1.37 Å, respectively. The presence of water has a clear effect on the adsorption energy, which increases to 1.3 eV. The O–O bond length is in the presence of water 1.44 Å, whereas the excess Bader charge is 0.84 e. The influence of water on the adsorption of  $O_2$  on Pt(111) is similar to Pd(111), with similar increases in adsorption energy, O–O bond length and charge transfer.

We find that the effect of water on the  $O_2$  adsorption energy is strongly metal dependent and that an enhanced adsorption energy correlates with an enhanced metal-to- $O_2$  charge transfer. The enhanced adsorption energy of  $O_2$  in the presence of water agrees with experimental temperature programmed desorption measurements for  $O_2$  desorption from Pd–Au alloys,<sup>[20]</sup> where the  $O_2$  desorption traces are shifted to higher temperatures in the presence of water.

In various reactions, it is possible to have both H and  $O_2$  on the surface. Thus, the question arises whether the transfer of  $H^+$  to the solution and simultaneous charging of the surface further enhances the  $O_2$  adsorption strength. We investigate this situation by artificially charging the surface slabs, see Figure 5. We find that the excess surface charge does not alter the adsorption properties of  $O_2$ . For all cases, the adsorption energy, excess Bader charge and O–O bond length are close to unaffected by the excess electron, thus,  $O_2$  adsorption in water is largely governed by hydrogen bonds.

## Conclusions

Using DFT calculations and *ab initio* molecular dynamics, we have investigated the effects of water on the adsorption properties of H and  $O_2$  over Cu(111), Ag(111), Au(111), Pd(111) and Pt(111). For H, we find that the formation of solvated  $H^+$  and a negatively charged metal surface is exothermic with respect to H adsorbed on the surface for Ag, Au and Pt.  $H^+$  solvation is close to thermo-neutral on Pd and endothermic on Cu. *Ab initio* molecular dynamics simulations show that the charge separation process is facile at room temperature, and for Au and Pt associated with free energy barriers around 0.3 eV and 0.4 eV, respectively. The spontaneous formation of solvated  $H^+$  is anticipated to have implications on the understanding of surface reactions at the metal-liquid interface. Reactions with surface species can in this case occur via pathways with solvated  $H^+$ , instead of H adsorbed on the surface. A different kind of charge separation is observed for  $O_2$  adsorption in the presence of water. The water- $O_2$  hydrogen bonds promote the metal-to- $O_2$  charge transfer, which results in an enhanced adsorption strength and an increased O–O bond length.

The results rationalize experimental finding and stress the need to account for charge separation effects when investigating catalytic reactions at the metal-liquid interface. Charge separation effects may modify the reaction energy landscape and give rise to alternative reaction pathways.

## Computational Details

Density functional theory calculations are performed, using the Vienna Ab initio Simulation Package (VASP).<sup>[38–41]</sup> To describe the interaction between the core and valence electrons, the project-augmented wave (PAW)<sup>[42,43]</sup> method is used. The considered valence electrons are  $1s^1$  (H),  $2s^2 2p^4$  (O),  $5s^1 4d^{10}$  (Ag),  $6s^1 5d^{10}$  (Au),  $4s^1 3d^{10}$  (Cu),  $5s^0 4d^{10}$  (Pd),  $6s^0 5d^{10}$  (Pt). The functional proposed by Perdew, Ernzerhof and Burke (PBE) is used,<sup>[44]</sup> together with the Grimme-D3 correction<sup>[45,46]</sup> to account for the van der Waals interactions. The Kohn-Sham orbitals are expanded in plane waves with a kinetic energy cut-off at 450 eV.

Structural relaxations and vibrational analyses are performed using  $p(3 \times 3)$  surface cells. The periodic slabs consist of six atomic layers, where the bottom two layers are fixed to their bulk positions to emulate a bulk system. For calculations without water, the slabs are separated by 14 Å of vacuum. The Brillouin zone is sampled using a  $\Gamma$ -centered (7,7,1) k-points mesh. The electronic structure is considered converged when the change of electronic energy and Kohn-Sham eigenvalues between two succeeding iterations are smaller than  $1 \cdot 10^{-6}$  eV. The structures are regarded converged when the forces on all nuclei are below 0.03 eV/Å. The lattice constants of Cu, Ag, Au, Pd, Pt are calculated to be 3.57 Å, 4.07 Å, 4.10 Å, 3.89 Å and 3.92 Å, respectively, which is in good agreement with the experimental values of 3.61 Å, 4.09 Å, 4.08 Å, 3.89 Å and 3.92 Å, respectively.<sup>[47]</sup> Gas phase  $H_2$  and  $O_2$  are described using a (30, 31, 32) Å box, sampled by the  $\Gamma$ -point. Harmonic vibrational modes are determined using the finite-differences approach.

*Ab initio* Molecular dynamics (AIMD) simulations are performed for water layers on  $p(3 \times 3)$  surface cells with and without adsorbates. The slabs are in these cases described by three atomic layers, with the bottom layer frozen and the k-point sampling restricted to a  $\Gamma$ -centered (3,3,1) mesh. Each slab is separated by 14 Å of water, with a  $H_2O$  density of 1 g/cm<sup>3</sup>. The electronic structure is in the AIMD simulations considered converged when the change in electronic energy and Kohn-Sham eigenvalues between two succeeding iterations are below  $1 \cdot 10^{-5}$  eV. The mass of H is set to 3 u and the time step to 1 fs. A target temperature of 20 °C is maintained using a Nosé-Hoover thermostat. The lowest energy structures obtained from 10 ps AIMD simulations are extracted and relaxed using slabs with six metal layers. The water layer has many local minima, which makes the evaluation of adsorption energies challenging. However, the trends in adsorption energies obtained from static calculations and AIMD coincide, which suggest that we have found the most relevant structures. The influence of excess charge in the metal on the adsorption of  $O_2$  is examined by artificially adding an additional electron to the surface slab with and without adsorbed  $O_2$ . The adsorption energy on the bare surface ( $E_{\text{ads}}^{\text{bare}}$ ) is calculated with respect to the bare surface and the gas phase molecules, whereas the adsorption energy in the presence of water ( $E_{\text{ads}}^{\text{H}_2\text{O}}$ ) is calculated with respect to the converged metal-water structure and the adsorbate in gas phase, *i.e.*,

$$E_{\text{ads}}^{\text{bare}}(\text{H}) = E_{\text{metal+H}} - E_{\text{metal}} - \frac{1}{2}E(\text{H}_2)$$

$$E_{\text{ads}}^{\text{bare}}(\text{O}_2) = E_{\text{metal+O}_2} - E_{\text{metal}} - E(\text{O}_2)$$

$$E_{\text{ads}}^{\text{H}_2\text{O}}(\text{H}) = E_{\text{metal+water+H}} - E_{\text{metal+water}} - \frac{1}{2}E(\text{H}_2)$$

$$E_{\text{ads}}^{\text{H}_2\text{O}}(\text{O}_2) = E_{\text{metal+water+O}_2} - E_{\text{metal+water}} - E(\text{O}_2)$$

All energies are reported with zero-point corrections for the adsorbates and the gas phase molecules.

## Acknowledgements

Financial support is acknowledged from the Swedish Research Council (2020-05191). The calculations were performed at NSC via a SNIC grant (2022/3-14). The Competence Centre for Catalysis (KCK) is hosted by Chalmers University of Technology and is financially supported by the Swedish Energy Agency and the member companies Johnson Matthey, Perstorp, Powercell, Preem, Scania CV, Umicore, and Volvo Group.

## Conflict of Interests

The authors declare no conflict of interest.

## Data Availability Statement

The data that support the findings of this study are available from the corresponding author upon reasonable request.

**Keywords:** density functional theory · charge-separation · charge transfer · metal-water interface · catalysis

- [1] R. Schlögl, *Angew. Chem. Int. Ed.* **2015**, *54*, 3465–3520.
- [2] D. Degerman, M. Shipilin, P. Lomker, C. M. Goodwin, S. M. Gericke, U. Hejral, J. Gladh, H. Y. Wang, C. Schlueter, A. Nilsson, et al. *J. Am. Chem. Soc.* **2022**, *144*, 7038–7042.
- [3] K. Reuter, M. Scheffler, *Phys. Rev. Lett.* **2003**, *90*, 046103.
- [4] J. K. Nørskov, T. Bligaard, J. Rossmeisl, C. H. Christensen, *Nat. Chem.* **2009**, *1*, 37–46.
- [5] J. K. Nørskov, F. Abild-Pedersen, F. Studt, T. Bligaard, *Proc. Nat. Acad. Sci.* **2011**, *108*, 937–943.
- [6] I. X. Green, W. Tang, M. Neurock, J. T. Yates Jr, *Science* **2011**, *333*, 736–739.
- [7] A. Bruix, J. T. Margraf, M. Andersen, K. Reuter, *Nat. Catal.* **2019**, *2*, 659–670.
- [8] B. W. Chen, L. Xu, M. Mavrikakis, *Chem. Rev.* **2020**, *121*, 1007–1048.
- [9] D. S. Potts, D. T. Bregante, J. S. Adams, C. Torres, D. W. Flaherty, *Chem. Soc. Rev.* **2021**, *50*, 12308–12337.
- [10] N. Dubouis, A. Grimaud, *Chem. Sci.* **2019**, *10*, 9165–9181.
- [11] S. Sharma, B. G. Pollet, *J. Power Sources* **2012**, *208*, 96–119.
- [12] C. Samanta, *Appl. Catal. A* **2008**, *350*, 133–149.
- [13] N. Yan, C. Xiao, Y. Kou, *Coord. Chem. Rev.* **2010**, *254*, 1179–1218.
- [14] V. Paunovic, V. V. Ordonsky, V. L. Sushkevich, J. C. Schouten, T. A. Nijhuis, *ChemCatChem* **2015**, *7*, 1161–1176.
- [15] P. J. Dyson, P. G. Jessop, *Catal. Sci. Technol.* **2016**, *6*, 3302–3316.
- [16] A. Santos, R. J. Lewis, G. Malta, A. G. Howe, D. J. Morgan, E. Hampton, P. Gaskin, G. J. Hutchings, *Ind. Eng. Chem. Res.* **2019**, *58*, 12623–12631.
- [17] J. S. Adams, A. Chemburkar, P. Priyadarshini, T. Ricciardulli, Y. Lu, V. Maliekkal, A. Sampath, S. Winikoff, A. M. Karim, M. Neurock, et al. *Science* **2021**, *371*, 626–632.
- [18] R. L. Augustine, R. W. Warner, M. J. Melnick, *J. Org. Chem.* **1984**, *49*, 4853–4856.
- [19] D. T. Limmer, A. P. Willard, P. Madden, D. Chandler, *Proc. Nat. Acad. Sci.* **2013**, *110*, 4200–4205.
- [20] S. Han, E. J. Evans, G. M. Mullen, C. B. Mullins, *Chem. Commun.* **2017**, *53*, 3990–3993.
- [21] Y. Sha, T. H. Yu, Y. Liu, B. V. Merinov, W. A. Goddard III, *J. Phys. Chem. Lett.* **2010**, *1*, 856–861.

- [22] J. K. Edwards, B. Salsona, E. Ntainjua N, A. F. Carley, A. A. Herzing, C. J. Kiely, G. J. Hutchings, *Science* **2009**, 323, 1037–1041.
- [23] T. Ricciardulli, S. Gorthy, J. S. Adams, C. Thompson, A. M. Karim, M. Neurock, D. W. Flaherty, *J. Am. Chem. Soc.* **2021**, 143, 5445–5464.
- [24] N. Kizhakevariam, E. Stuve, *Surf. Sci.* **1992**, 275, 223–236.
- [25] N. M. Wilson, D. W. Flaherty, *J. Am. Chem. Soc.* **2016**, 138, 574–586.
- [26] Z. Zhao, R. Bababrik, W. Xue, Y. Li, N. M. Briggs, D.-T. Nguyen, U. Nguyen, S. P. Crossley, S. Wang, B. Wang, et al. *Nature Catalysis* **2019**, 2, 431–436.
- [27] J. S. Adams, M. L. Kromer, J. Rodríguez-L'opez, D. W. Flaherty, *J. Am. Chem. Soc.* **2021**, 143, 7940–7957.
- [28] R. Svensson, H. Gronbeck, *J. Am. Chem. Soc.* **2023**, 145, 11579–11588.
- [29] Q. Zhang, A. Asthagiri, *Catal. Today* **2019**, 323, 35–43.
- [30] M. Valter, B. Wickman, A. Hellman, *J. Phys. Chem. C* **2021**, 125, 1355–1360.
- [31] D. Lackey, J. Schott, J.-K. Sass, S.-I. Woo, F. Wagner, *Chem. Phys. Lett.* **1991**, 184, 277–281.
- [32] M. Pan, Z. D. Pozun, W.-Y. Yu, G. Henkelman, C. B. Mullins, *J. Phys. Chem. Lett.* **2012**, 3, 1894–1899.
- [33] H. L. Skriver, N. Rosengaard, *Phys. Rev. B* **1992**, 46, 7157.
- [34] G. Tawa, I. Topol, S. Burt, R. Caldwell, A. Rashin, *J. Chem. Phys.* **1998**, 109, 4852–4863.
- [35] J. Heras, L. Viscido, *Appl. Surf. Sci.* **1980**, 4, 238–241.
- [36] M. Sprik, G. Ciccotti, *J. Chem. Phys.* **1998**, 109, 7737–7744.
- [37] L. Chen, J. W. Medlin, H. Gronbeck, *ACS Catal.* **2021**, 11, 2735–2745.
- [38] G. Kresse, J. Hafner, *Phys. Rev. B* **1993**, 47, 558.
- [39] G. Kresse, J. Hafner, *Phys. Rev. B* **1993**, 48, 13115.
- [40] G. Kresse, J. Hafner, *Phys. Rev. B* **1994**, 49, 14251.
- [41] G. Kresse, J. Furthmüller, *Phys. Rev. B* **1996**, 54, 11169.
- [42] P. E. Blöchl, *Phys. Rev. B* **1994**, 50, 17953.
- [43] G. Kresse, D. Joubert, *Phys. Rev. B* **1999**, 59, 1758.
- [44] J. P. Perdew, K. Burke, M. Ernzerhof, *Phys. Rev. Lett.* **1996**, 77, 3865.
- [45] S. Grimme, J. Antony, S. Ehrlich, H. Krieg, *J. Chem. Phys.* **2010**, 132, 154104.
- [46] S. Grimme, S. Ehrlich, L. Goerigk, *J. Comb. Chem.* **2011**, 32, 1456–1465.
- [47] J. R. Rumble, Ed. "Crystal Structures and Lattice Parameters of Allotropes of the Elements" in *Handbook of Chemistry and Physics*, 104<sup>th</sup> ed.; CRC Press, Inc., 2023.

---

Manuscript received: February 1, 2024

Accepted manuscript online: February 5, 2024

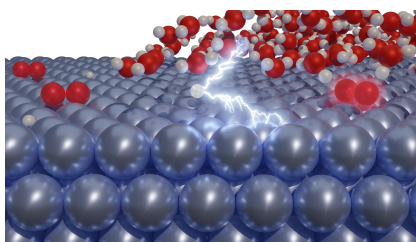
Version of record online: ■■, ■■

## RESEARCH ARTICLE

---

Density functional theory calculations and free energy simulations show a spontaneous charge separation of hydrogen atoms at metal-water interfaces, where a proton is solvated in the water structure, and an electron is donated to the metal surface. Moreover, the presence of water gives rise to a significant metal-to-O<sub>2</sub> charge transfer, increasing the adsorption strength as compared to the adsorption in the absence of water.

---



*R. Svensson\**, *H. Grönbeck\**

1 – 8

**Spontaneous Charge Separation at the Metal-Water Interface**

